Electronic Supplement 7

Conversion from spectral radiance to lava area, heat flux and discharge rate

This electronic supplement is modified from an exercise designed for a Masters level class in thermal remote sensing. The exercise uses two NOAA-16 AVHRR images of Etna acquired during a period of active lava flow. These are given as the two 13 bit image files attached to this electronic supplement, where:

- the file named "29may010046etbt4.13bit" is the channel 4 image acquired on 29 May 2001 at 0046Z, and
- the file named "30may010036etbt4.13bit" is the channel 4 image acquired on 30 May 2001 at 0036Z.

Also given are the image information files (in text format) for the two images. The information files give the channel 4 image information, including:

- satellite information [NOAA-16: orbit direction – ascending (S-N) or descending (N-S)];
- pixel dimension;
- calibration coefficients (i.e., the gain, or slope, and intercept used for the linear conversion between DN and spectral radiance), and
- the blackbody temperature (necessary for application of the non-linearity correction to the DN conversion).

Electronic Supplement 2 explains how these values are used for calibration, i.e., to convert the DN to spectral radiance. These data were acquired at the University of Dundee (Dundee, Scotland) receiving station, and then processed (and provided) by the NERC Earth Observation Data Acquisition and Analysis Service (NEODAAS) at the Plymouth Marine Laboratory (Plymouth, UK). Processing by NEODAAS involved geometric correction, as well as calibration (including correction for non-linearity) and conversion to brightness temperature.

The exercise is designed to allow application of the following five steps commonly applied to process volcano hot spot data in AVHRR data:

Step 1: Hot spot identification and extraction of relevant pixel radiance data;
Step 2: Application of atmospheric and emissivity corrections;
Step 3: Application of a mixture model to extract sub-pixel hot spot size;
Step 4: Conversion to lava area and heat flux; and, ultimately,
Step 5: Conversion to lava discharge rate.

The images used for the exercise are given in Figures S7.1 and S7.2. Both show a hot spot at the summit of Mt. Etna which is sufficiently intense to cause a four to five pixel thermal anomaly in the TIR band (channel 4) in both images. Data are unsaturated. It is these unsaturated channel 4 data with which we will work. For this case, the MIR band (channel 3) data are not available, but the AVHRR MIR band is usually saturated over pixels containing active lava (see Electronic Supplement 1), meaning that this is a fairly typical case (i.e., we have only one band in the TIR with which we can work). As a result, the exercise demonstrates a "standard" methodology as applied to AVHRR-class data for hot spot parameter extraction.

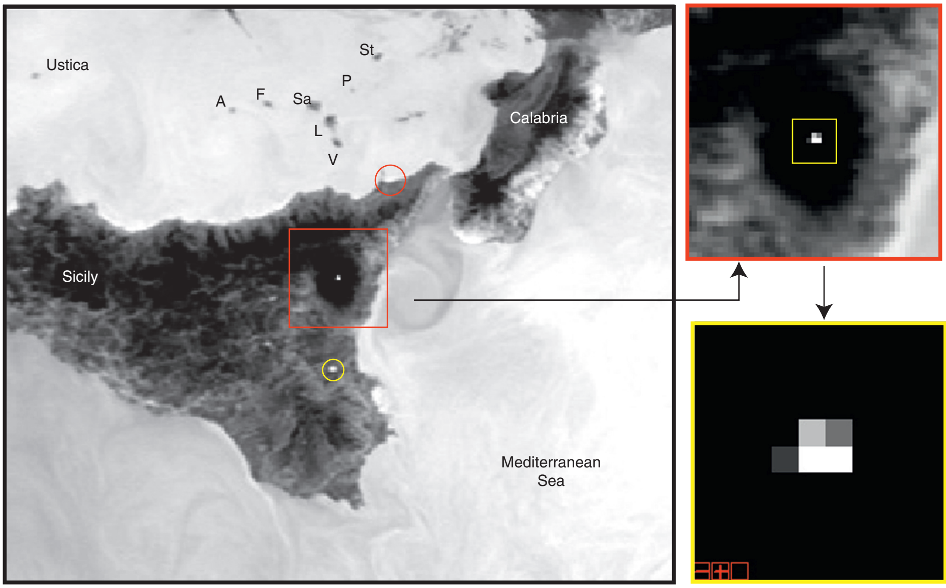

Figure S7.1 AVHRR channel 4 sub-image of Sicily and Calabria obtained at 00:46Z on 29 May 2001. Sub-image is 320 × 300 pixels, or ~350 × 330 km, in size. Lighter tones indicate higher pixel-integrated temperatures. The Aeolian islands of Alicudi, Filicudi, Salina, Lipari, Vulcano, Panarea and Stromboli are labeled using the first letter of each islands name. The oil refinery at, and cape of, Milazzo are located using the red circle (the oil refinery registers a hot spot in the AVHRR MIR and TIR bands). Yellow circle contains an "apparent" hot spot due to the presence of a lake (Biviere di Lentini) which appears relatively warm by night (against the cool land background) and relatively cool by day (against the warm, solar-heated, land background). Note that the real hot spot on Etna is somewhat crisper (more cleanly defined) than the fuzzier "apparent" hot spot of the lake, and two other lake-related "apparent" hot spots can be seen to the SW of Etna. Mount Etna is located using the red box, and is magnified top right. In this nighttime image, the sea (like the lake) is relatively warm (lighter tones) compared with the land (darker tones), and Etna is apparent as a cold, circular, feature (due to its elevation, surface temperatures decrease with height causing the volcano to appear as a cold zone). The hot spot at Etna's summit is centered in the yellow box and magnified lower right. The hot spot is due to pixels containing active lava, and is obvious as a group of hot (white) pixels against a cold (black) background. The lava channel contained in these 1 km pixels is pictured in Figure S7.5.

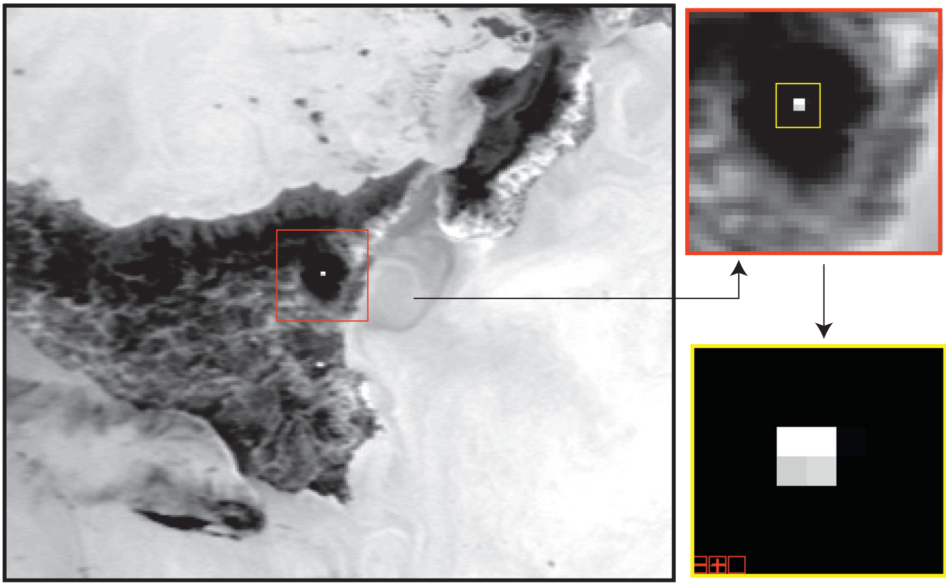

Figure S7.2 AVHRR channel 4 sub-image of Sicily and Calabria obtained at 00:36Z on 30 May 2001. See caption of Figure S7.1 for explanation.

The exercise

For this exercise we will use data from two AVHRR images acquired during an effusive eruption at Mt. Etna (Sicily, Italy). The image contains a thermal anomaly due to the presence of active lava flows near the summit of the volcano. The images were acquired on 29 May 2001 at 00:46Z and on 30 May 2001 at 00:36Z. Just after the two images were acquired we carried out field work at the active lava flow field contained within the pixels imaged during the two over-passes. Our field observations revealed a lava flow field active over an area of 2.5 × 1.0 km, consistent with the 3 pixel by 2 pixel (i.e., 3.3 km × 2.2 km) size of the thermal anomaly in the two (1 km spatial resolution) images. We use our field measurements (given at the end of the exercise) to check the discharge rate values extracted from the two images.

Both images are actually 320 × 300 pixel sub-images centered on Mt. Etna (i.e., they cover just a portion of the full 2048 × 2048 pixel AVNRR image). They also cover the Aeolian Islands (including the active volcanoes of Vulcano and Stromboli, as located in Figure S7.1). The objective of the practical is to set up a spreadsheet to allow calculation of lava area, heat flux and discharge rate using the AVHRR TIR data. To achieve this we apply the five image processing and data conversion steps given in sequence as part of the practical. The 5 × 4 pixel brightness temperature grid centered on each hot spot, as extracted and used in these steps, is given Figure S7.3, on which the area of the thermal anomaly is also marked.

(a) 29 May 2001, 0046Z

30 85	27 45	23 40	24 38	28 64
30 05	33 50	46 82	43 81	32 40
32 24	41 80	60 31	53 73	34 32
29 95	31 52	35 29	33 14	30 26

(b) 30 May 2001, 0036Z

32 77	33 20	32 14	31 74	32 40
40 64	49 22	49 36	42 06	36 27
40 56	47 62	47 90	41 41	36 67
29 52	28 09	29 24	32 79	34 87

Figure S7.3 Pixel grids of AVHRR channel 4 brightness temperature centered on the Etna summit hot spot for (a) the 29 May, and (b) the 30 May 2001 sub-images. Values are brightness temperature plus 30 °C multiplied by 100. Area of the anomaly is marked by the red line, with a potential extra "anomalous" pixel on the 30 May being highlighted in yellow. Inclusion of this pixel increases the volume flux estimate from 1.7 – 2.1 $m^3 s^{-1}$ to 2.0 – 2.3 $m^3 s^{-1}$.

Step 1: Selection of hot (thermally anomalous) pixels

Use ENVI to open the channel 4 (10.3 – 11.3 μm) AVHRR image and identify the anomalous pixels.

To do this you need to:

(1) Use the "*Open Image File*" function to open the image. The image dimensions can be found in the *.*info* file for the image.
Note: the data format are **Integer, ENVI Standard, Network (IEEE)**

(2) Find the thermal anomaly (hot spot) on Mt. Etna.

(3) Read off the pixel values for the anomalous (hot spot) pixels using the "*Cursor location / Value*" function available in the "*Tools*" menu.

(4) Read off the appropriate background values. To do this identify the nearest pixels to the anomaly (i.e., any dark, cold, pixels surrounding the anomaly). Take the minimum value from the dark, cold pixels immediately surrounding each anomalous (light, hot) pixel. The "hot" and "cold" pixel combinations selected are given in Figure S7.4, where I have selected the minimum "cold" pixel value immediately surrounding each hot pixel in the cardinal and diagonal directions.

(5) Enter the brightness temperature for each anomalous pixel and its background temperature into the appropriate columns in the data entry and conversion spreadsheet, as given in Table S7.1.
Note:
Pixel values are not DN or spectral radiance. Instead they are values (x) that can be converted to brightness temperature in degrees centigrade by dividing by 100 and subtracting 30 from the result, i.e.,

$$T^* = (x/100) - 30 \qquad (°C)$$

Therefore, to obtain brightness temperature (T*) in Kelvin divide the pixel value by 100, subtract 30 and add 273.15.

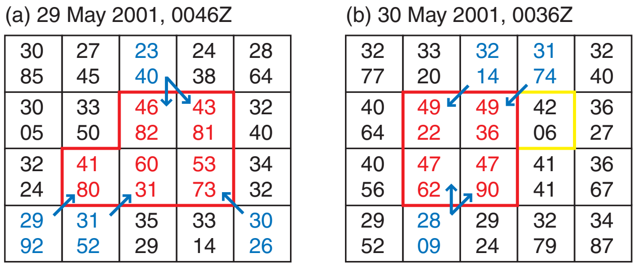

Figure S7.4 Pixel grids of AVHRR channel 4 brightness temperature centered on the Etna summit hot spot for (a) the 29 May, and (b) the 30 May 2001 sub-images. Values defined within the hot spot are given in red, and "cold" background pixels are given in blue; these are linked to the "hot" pixels for which they are used to characterize the background temperature (T_a) in the mixture model using blue arrows.

The remaining processing steps involve a series of conversions. We will use the EXCEL spreadsheet template of Table S7.1 to complete these conversions by entering each of the following conversions into the sheet in sequence (column by column).

Step 2: Correction for atmospheric and emissivity effects

(1) To execute the atmospheric and emissivity corrections, we first need to convert each brightness temperature to a spectral radiance. For the AVHRR sensor, spectral radiances are recorded in units of milliwatts/m^2-steradian-cm^{-1}. Thus, wavelength needs to be entered into the Planck Function as a wavenumber in cm^{-1}, c_1 will be 1.191 × 10^{-5} mW sr^{-1} cm^{-4} and c_2 is 1.439 cm K. The Planck Function for spectral radiance also needs to be modified to:

$$L(v, T) = c_1 v^3 \left[\exp^{\frac{c_2 v}{T}} - 1\right]^{-1} \quad (\mathrm{mW\ sr^{-1}\ m^{-2}\ cm^{-1}})$$

v being wavenumber (in cm^{-1}). Thus, three microns (3 µm) becomes $\frac{1}{0.0003\mathrm{cm}}$ or 3333 cm^{-1}, and for a temperature of 290 K, we obtain a spectral radiance of

$$L(\lambda, \mathrm{T}) = (1.191\mathrm{x}10^{-5}\ \mathrm{mWsr^{-1}\ cm^{-4}})(3333\mathrm{cm^{-1}})^3 \left(\exp^{\frac{(1.439\mathrm{cmK})(3333\mathrm{cm^{-1}})}{(290\mathrm{K})}} - 1\right)^{-1}$$
$$= 0.0289\ \mathrm{mW\ sr^{-1}\ m^{-2}\ cm^{-1}}$$

Note:
Temperature must be input in Kelvin, and wavelength in cm^{-1}.

(2) Next, we need to correct each hot spot and background spectral radiance for emissivity and atmospheric effects. Given that we are working in the TIR, we can use the following correction taken from Electronic Supplement 4:

Table S7.1a *Data entry and conversion spreadsheet for the "cold model", i.e., pixel mixture model applied with assumption that lava surface (T_c) is at 100 °C. First row and last column give EXCEL row and line coordinates.*

A	B	C	D	E	F	G	H	I	J	K	L	1
Temperature Case 1:			**100**	**C**		**273.23**	**mW sr^{-1} m^{-2} cm^{-1}**			**(Cold Model)**		**2**
Brightness Temperature			$M(\lambda_{TIR},T^*)$,			$M(\lambda_{TIR},T_{int})$,				Active Lava		**3**
(°C)			(mW sr^{-1} m^{-2} cm^{-1})			(mW sr^{-1} m^{-2} cm^{-1})			Area (m^2)	Φ_{rad} (W)	Φ_{conv} (W)	**4**
Anomaly	Background		Anomaly	Background		Anomaly	Background					**5**
												6
												7
												8
												9
												10
												11
								Sum				**12**
												13
									Φ_{tot}		W	**14**
									V_R		m^3 s^{-1}	**15**
												16

Table S7.1b *Data entry and conversion spreadsheet for the "hot model", i.e., pixel mixture model applied with assumption that lava surface (T_c) is at 500 °C. First row and last column give EXCEL row and line coordinates.*

A	B	C	D	E	F	G	H	I	J	K	L	1
Temperature Case 2:			**500**	**C**		**2060.63**	**mW sr^{-1} m^{-2} cm^{-1}**			**(Hot Model)**		**2**
Brightness Temperature			M(λ_{TIR},T*),			M(λ_{TIR},T_{int}),				Active Lava		**3**
(°C)			(mW sr^{-1} m^{-2} cm^{-1})			(mW sr^{-1} m^{-2} cm^{-1})			Area (m^2)	Φ_{rad} (W)	Φ_{conv} (W)	**4**
Anomaly	Background		Anomaly	Background		Anomaly	Background					**5**
												6
												7
												8
												9
												10
												11
								Sum				**12**
												13
									Φ_{tot}		W	**14**
									V_R		m^3 s^{-1}	**15**
												16

$$M(\lambda_{TIR}, T_{int}) = [M(\lambda_{TIR}, T_{int}{}^{*}) \ - \ L_U(\lambda_{TIR})] \ / \tau_{\lambda TIR} \ \varepsilon_{\lambda TIR}$$

in which

$M(\lambda_{TIR}, T_{int}{}^{*})$ = Spectral radiance at wavelength λ_{TIR} for brightness temperature T*;
$L_U(\lambda_{TIR})$ = Atmospheric upwelling radiance at wavelength λ_{TIR};
$\tau_{\lambda TIR}$ = Atmospheric transmissivity at wavelength λ_{TIR};
$\varepsilon_{\lambda TIR}$ = Surface emissivity at wavelength λ_{TIR};
$M(\lambda_{TIR},T_{int})$ = Corrected spectral radiance for a pixel at integrated temperature of T_{int}.

For the surface type here (Etna basalt) and waveband (AVHRR channel 4), Table S4.2a of Electronic Supplement 4 gives $\varepsilon_{\lambda TIR}$ = 0.96. For our elevation (2000–3000 m), scan angle (nadir) and waveband (10.3–11.3 μm), Table S4.4 of Electronic Supplement 4 gives:

$\tau_{\lambda TIR}$ = 0.95
$L_u(\lambda)$ = 4.5 mW sr^{-1} m^{-2} cm^{-1}

This allows us to apply the model (MODTRAN)-based atmospheric correction as given above.

Step 3: Selection and application of an appropriate mixture model

Because we only have one band of data in the TIR, we are forced to apply the two component TIR solution of Chapter 4 (Section 4.3.1.2), i.e.,

$$p = \frac{M(\lambda_{TIR}, T_{\text{int}}) - M(\lambda_{TIR}, T_a)}{M(\lambda_{TIR}, T_c) - M(\lambda_{TIR}, T_a)}$$

in which

$M(\lambda_{TIR},T_{int})$ = corrected spectral radiance for pixel at integrated temperature of T_{int}.
$M(\lambda_{TIR},T_a)$ = spectral radiance for a surface at ambient temperature, T_a.
$M(\lambda_{TIR},T_c)$ = spectral radiance for a surface at active (crusted) lava temperature, T_c.
p = portion of the pixel occupied by hot, active (crusted) lava at temperature T_c.

To solve this equation we use the atmospherically corrected temperature for the background pixel temperature for T_a, and we need to assume a temperature for the surface of the hot active (crusted) lava at T_c. We then need to convert both of these temperatures to spectral radiances. We typically assume two end-member cases:

(1) Cold Model: Lava surface (T_c) = 100 °C, and
(2) Hot Model: Lava surface (T_c) = 500 °C.

These need to be converted to spectral radiances in mW sr^{-1} m^{-2} cm^{-1} at the AVHRR channel 4 wavelength (note that our atmospherically corrected background values should already be in the appropriate spectral radiance values).

Note:
The Equation will only work if we use radiances, and the radiance units need to be consistent, i.e., mW sr^{-1} m^{-2} cm^{-1}.

Step 4: Lava area and heat flux extraction

For each pixel, use p to convert to sub-pixel hot spot area (in m^2) as occupied by surfaces at (1) 100 °C and (2) 500 °C. To do this, we multiply by pixel area (A_{pixel}) which, from the image information file, we see has a value of 1.102357 × 1.102357 km,

$$A_c = pA_{pixel}$$

A_c is now the area of hot active (crusted) lava in each pixel.

Now sum the areas obtained for each hot spot pixel to obtain an estimate for the total lava area (A_{lava}). We will have one value for the cold model and a second value for the hot model, where A_{lava} for the cold model should be much greater than that for the hot model.

Next, calculate the heat flux due to radiation and convection for each pixel using,

$$\Phi_{rad} = A_c \varepsilon \sigma T_c{}^4$$

and

$$\Phi_{conv} = A_c h_c (T_c - T_a)$$

Here:
- ε = Surface emissivity
- σ = Stefan-Boltzmann constant
- h_c = Convective heat transfer coefficient

Note:
Temperature must be input in Kelvin, and area in m^2.

Again, sum the fluxes obtained for each pixel to obtain an estimate for the total heat flux (Φ_{tot}), where we will have one value for the cold model and a second value for the hot model. The Φ_{tot} for the cold model should be less than that for the hot model.

Step 5: Volume flux conversion

Now, Φ_{tot} can be used to estimate the lava volume flux (V_R, in m^3 s^{-1}) necessary to generate such a heat flux from:

$$V_R = \frac{\Phi_{tot}}{\rho(c_p \Delta T + L \Delta \phi)}$$

Here:

ρ = Lava bulk density (i.e., the dense rock value corrected for vesicularity).

c_p = Lava bulk heat capacity (i.e., the dense rock value corrected for vesicularity).

ΔT = Difference in temperature for the lava flow core at the vent and the point at which the flow core cools to a point at which further forward motion is rheologically impossible.

c_L = Latent heat of crystallization.

$\Delta\phi$ = Crystallization (expressed as a fraction) caused by cooling through ΔT.

Following Wright *et al*. (2001), V_R is likely a time-averaged lava discharge rate or TADR, i.e., the discharge rate averaged over the period of time required to attain the detected lava area. That is, the emplacement of the imaged lava area is not instantaneous, so it must be the result of some precedent rate of lava output whose level was sufficient to generate the lava area active at the time of image acquisition. The assumption is that, the higher the rate of supply, the greater the flow area, and the relation between supply and area is positive and linear.

We can apply this equation with the appropriate values from Table S7.2.

Note:

For convenience, use the mid-point values from Tables S7.2, e.g.,

For Etna, the range for c_p is 810 – 1035 J kg^{-1} K^{-1},
Thus use [(810 + 1035) /2] = 922.5 J kg^{-1} K^{-1}

(see Table 7.3 for values used to obtain answer key).

We arrive at two volume flux estimates, one for the hot model and one for the cold model; we assume that the actual value is located somewhere between the two.

Answer

The completed spreadsheet (i.e., the answer key) is given in Table S7.4 for the 29 May image, and in Table S7.5 for the 30 May image. The EXCEL-format equations entered into each cell of these spreadsheets (to achieve the conversions written out above and results of Tables S7.4 and S7.5) are given in Table S7.6.

Validation

During 30 May 2001 we made field measurements of the lava flow active within the AVHRR pixels imaged here [as published in Bailey *et al*. (2006)]. During five hours in the afternoon of 30 May we made repeated measurements of master channel depth (d), width (w) and

Table S7.2. *Constants used to convert between satellite TIR spectral radiance and heat-or-volume flux at Kilauea, Etna, Krafla, Stromboli and Santiaguito.*

Parameter	Kilauea	Etna	Krafla	Stromboli	Santiaguito
T_c (°C)	100 – 500	100 – 500	100 – 500	100 – 500	125 – 250
T_a (°C)	35	0	0	0	20
σ (W m^{-2} K^{-4})	5.67×10^{-8}	5.67×10^{-8}	5.67×10^{-8}	5.67×10^{-8}	5.67×10^{-8}
h_c (W m^{-2} K^{-1})	0	~10	~10	~10	35 – 75
DRE ρ (kg m^{-3})	2600±100	2600	2600	2600	2600
DRE c_p (J kg^{-1} K^{-1})	1225	1150	1150	1150	1150
Vesicularity (%)	10 – 40	10 – 34	10 – 34	10 – 22	10 – 30
Bulk ρ (kg m^{-3})	1560 – 2340	1720 – 2340	1720 – 2340	2030 – 2340	1820 – 2340
Bulk c_p (J kg^{-1} K^{-1})	735 – 1100	810 – 1035	810 – 1035	900 – 1035	805 – 1035
ΔT (K)	315 – 385	200 – 350	200 – 350	200 – 350	200 – 330
$\Delta\phi$ (%)	2 – 45	45	45	45	0 – 45
c_L (J kg^{-1})	3.5×10^5	3.5×10^5	3.5×10^5	3.5×10^5	3.5×10^5

[from Table 2 of Harris *et al*. (2007): "values used to calibrate the thermal approach (conversion of satellite radiance to volume flux) at Kilauea (Harris *et al*., 1998), Etna (Harris *et al*., 2000), Krafla (Harris *et al*., 2000), Stromboli (Calvari *et al*., 2005) and Santiaguito (Harris *et al*., 2003)"]

Sources:

Calvari, S., Spampinato, L., Lodato, L., Harris, A.J.L., Patrick, M.R., Dehn, J., Burton, M.R. and Andronico, D. (2005). Chronology and complex volcanic processes during the 2002–2003 flank eruption at Stromboli volcano (Italy) reconstructed from direct observations and surveys with a handheld thermal camera. *Journal of Geophysical Research*, **110**, B02201. DOI: 10.1029/2004JB003129

Harris, A.J.L., Flynn, L.P., Keszthelyi, L., Mouginis-Mark, P.J., Rowland, S.K. and Resing, J.A. (1998). Calculation of Lava Effusion Rates from Landsat TM Data. *Bulletin of Volcanoogy*, **60**, 52–71.

Harris, A.J.L., Murray, J.B., Aries, S.E., Davies, M.A., Flynn, L.P., Wooster, M.J., Wright, R. and Rothery, D.A. (2000). Effusion rate trends at Etna and Krafla and their implications for eruptive mechanisms. *Journal of Volcanology and Geothermal Research*, **102**(3–4), 237–269.

Harris, A.J.L., Flynn, L.P. and Rose, W.I. (2003). Temporal trends in Lava Dome Extrusion at Santiaguito 1922–2000. *Bulletin of Volcanology*, **65**, 77–89.

velocity (u) within 50 m of the vent. By multiplying these three parameters we gained an independent estimation of the lava volume flux (i.e., V_R = dwu). Forty-nine measurements of velocity were made between 13:45Z and 17:38Z on 30 May, the last measurement being made ~7 hours before the satellite overpass. The channel width was 3 m. Maximum flow

Table S7.3 *Values used to obtain results given in answer key of Table S7.4.*

Model Input Parameter	Value	Units
Central Wave number	929	cm^{-1}
Emissivity	0.96	
Transmissivity	0.95	
Upwelling Radiance	4.5	$mW\ sr^{-1}\ m^{-2}\ cm^{-1}$
Pixel area	1214404	m^2
Convective heat transfer coefficient	10	$W\ m^{-2}\ K^{-1}$
Density	2030	$kg\ m^{-2}$
Specific heat capacity	922.5	$J\ kg^{-1}\ K^{-1}$
Cooling	275	C
Latent heat of crystallization	350000	$J\ kg^{-1}$
Crystallization	0.45	fraction

velocity (u_{max}) was somewhat variable, varying between 0.15 m s^{-1} and 0.87 m s^{-1}, with a mean and standard deviation of 0.46 m s^{-1} and 0.13 m s^{-1}. To calculate the flux of lava flowing in the channel we need to use mean velocity (u_{mean}), which can be approximated from $u_{mean} = 0.67u_{max}$.

If we use the lowest velocity obtained during the control period, we have a mean flow velocity of,

$$u_{mean} = 0.67(0.15\ \mathrm{m\ s^{-1}}) = 0.10\ \mathrm{m\ s^{-1}}$$

Given a semi-circular channel of radius 1.5 m, this yields a volume flux of,

$$V_R = \pi(1.5\ \mathrm{m})^2(0.58\ \mathrm{m\ s^{-1}}) = 0.7\ \mathrm{m^3 s^{-1}},$$

which corrected for a vesicularity of 0.22 gives a bulk volume flux of,

$$V_R = (1-0.22)(4.1\ \mathrm{m^3 s^{-1}}) = 0.6\ \mathrm{m^3 s^{-1}}.$$

If we use the highest velocity obtained during the control period, we have a mean flow velocity of,

$$u_{mean} = 0.67(0.87\ \mathrm{m\ s^{-1}}) = 0.58\ \mathrm{m\ s^{-1}}$$

Table S7.4a *Answer key for the "cold model" for the 29 May image (anomaly and background values entered are those indicated in Figure S7.4a). First row and last column give EXCEL row and line coordinates.*

A	**B**	**C**	**D**	**E**	**F**	**G**	**H**	**I**	**J**	**K**	**L**	**1**
Temperature Case 1:			**100**	**C**		**273.23**	**mW sr^{-1} m^{-2} cm^{-1}**			**(Cold Model)**		**2**
Brightness Temperature			$M(\lambda_{TIR},T^*)$,			$M(\lambda_{TIR},T_{int})$,				Active Lava		**3**
(°C)			(mW sr^{-1} m^{-2} cm^{-1})			(mW sr^{-1} m^{-2} cm^{-1})			Area (m^2)	Φ_{rad} (W)	Φ_{conv} (W)	**4**
Anomaly	Background		Anomaly	Background		Anomaly	Background					**5**
11.8	−0.08		88.46	72.01		92.06	74.02		1.10E+05	1.16E+08	1.10E+08	**6**
30.31	1.52		118.13	74.11		124.59	76.32		2.98E+05	3.14E+08	2.93E+08	**7**
23.73	0.26		107.02	72.45		112.41	74.51		2.32E+05	2.44E+08	2.31E+08	**8**
13.81	−6.6		91.44	63.83		95.33	65.05		1.77E+05	1.86E+08	1.88E+08	**9**
16.82	−6.6		96.02	63.83		100.35	65.05		2.06E+05	2.17E+08	2.20E+08	**10**
												11
								Sum	1.02E+06	1.08E+09	1.04E+09	**12**
												13
									Φ_{tot}	2.12E+09	W	**14**
									V_R	2.5	m^3 s^{-1}	**15**
												16

Table S7.4b *Answer key for the "hot model" for the 29 May image (anomaly and background values entered are those indicated in Figure S7.4a). First row and last column give EXCEL row and line coordinates.*

A	B	C	D	E	F	G	H	I	J	K	L	1
Temperature Case 2:			**500**	**C**		**2060.63**	**mW sr^{-1} m^{-2} cm^{-1}**			**(Hot Model)**		**2**
Brightness Temperature			$M(\lambda_{TIR},T^*)$,			$M(\lambda_{TIR},T_{int})$,				Active Lava		**3**
(°C)			(mW sr^{-1} m^{-2} cm^{-1})			(mW sr^{-1} m^{-2} cm^{-1})			Area (m^2)	Φ_{rad} (W)	Φ_{conv} (W)	**4**
Anomaly	Background		Anomaly	Background		Anomaly	Background					**5**
11.8	−0.08		88.46	72.01		92.06	74.02		1.10E+04	2.14E+08	5.51E+07	**6**
30.31	1.52		118.13	74.11		124.59	76.32		2.95E+04	5.75E+08	1.47E+08	**7**
23.73	0.26		107.02	72.45		112.41	74.51		2.32E+04	4.51E+08	1.16E+08	**8**
13.81	−6.6		91.44	63.83		95.33	65.05		1.84E+04	3.58E+08	9.34E+07	**9**
16.82	−6.6		96.02	63.83		100.35	65.05		2.15E+04	4.18E+08	1.09E+08	**10**
												11
								Sum	1.04E+05	2.02E+09	5.20E+08	**12**
												13
									Φ_{tot}	2.54E+09	W	**14**
									V_R	3.0	m^3 s^{-1}	**15**
												16

Table S7.5a *Answer key for the "cold model" for the 30 May image (anomaly and background values entered are those indicated in Figure S7.4b). First row and last column give EXCEL row and line coordinates.*

A	B	C	D	E	F	G	H	I	J	K	L	1
Temperature Case 1:			**100**	**C**		**273.23**	**mW sr^{-1} m^{-2} cm^{-1}**			**(Cold Model)**		**2**
Brightness Temperature			M(λ_{TIR},T*),			M(λ_{TIR},T_{int}),				Active Lava		**3**
(°C)			(mW sr^{-1} m^{-2} cm^{-1})			(mW sr^{-1} m^{-2} cm^{-1})			Area (m^2)	Φ_{rad} (W)	Φ_{conv} (W)	**4**
Anomaly	Background		Anomaly	Background		Anomaly	Background					**5**
19.22	2.14		99.76	74.93		104.45	77.23		1.69E+05	1.78E+08	1.65E+08	**6**
19.36	1.74		99.98	74.40		104.70	76.64		1.73E+05	1.83E+08	1.70E+08	**7**
17.62	−1.91		97.26	69.65		101.71	71.44		1.82E+05	1.92E+08	1.86E+08	**8**
17.9	−1.91		97.69	69.65		102.19	71.44		1.85E+05	1.95E+08	1.89E+08	**9**
												10
												11
								Sum	7.09E+05	7.48E+08	7.10E+08	**12**
												13
									Φ_{tot}	1.46E+09	W	**14**
									V_R	1.7	m^3 s^{-1}	**15**
												16

Table S7.5b *Answer key for the "hot model" for the 30 May image (anomaly and background values entered are those indicated in Figure S7.4b). First row and last column give EXCEL row and line coordinates.*

A	B	C	D	E	F	G	H	I	J	K	L	1
Temperature Case 2:			**500**	**C**		**2060.63**	**mW sr^{-1} m^{-2} cm^{-1}**			**(Hot Model)**		**2**
Brightness Temperature			$M(\lambda_{TIR},T^*)$,			$M(\lambda_{TIR},T_{int})$,				Active Lava		**3**
(°C)			(mW sr^{-1} m^{-2} cm^{-1})			(mW sr^{-1} m^{-2} cm^{-1})			Area (m^2)	Φ_{rad} (W)	Φ_{conv} (W)	**4**
Anomaly	Background		Anomaly	Background		Anomaly	Background					**5**
19.22	2.14		99.76	74.93		104.45	77.23		1.67E+04	3.24E+08	8.30E+07	**6**
19.36	1.74		99.98	74.40		104.70	76.64		1.72E+04	3.34E+08	8.56E+07	**7**
17.62	−1.91		97.26	69.65		101.71	71.44		1.85E+04	3.59E+08	9.28E+07	**8**
17.9	−1.91		97.69	69.65		102.19	71.44		1.88E+04	3.65E+08	9.42E+07	**9**
												10
												11
								Sum	7.11E+04	1.38E+09	3.56E+08	**12**
												13
									Φ_{tot}	1.74E+09	W	**14**
									V_R	2.1	m^3 s^{-1}	**15**
												16

Table S7.6 *EXCEL format Equations entered into row 6 of the "data entry and conversion" spreadsheet of Table 7.1.*

Conversion	Cell location (for Equation)	EXCEL Equation
Image value to brightness temperature conversion	Anomaly value: A6	= (4180/100) – 30
	Background value: B6	= (2992/100) – 30
Brightness temperature to spectral radiance conversion	Anomaly value: D6	=0.000011910659*929^3/((EXP (1.438833*929/(A6+273.15)))-1)
	Background value: E6	=0.000011910659*929^3/((EXP (1.438833*929/(B6+273.15)))-1)
Atmospheric correction	Anomaly value: G6	= (D6 – 4.5) / (0.96*0.95)
	Background value: H6	= (E6 – 4.5) / (0.96*0.95)
Sub-pixel area calculation	J6	=((G6-H6)/(G2-H6))*1214404
Radiative heat flux	K6	=J6*(0.00000005670.96*(D2 +273.15)^4)
Convective heat flux	L6	=J6*10*(D2-B6)

Given a semi-circular channel of radius 1.5 m, this yields a volume flux of,

$$V_R = \pi(1.5\ \text{m})^2(0.58\ \text{m s}^{-1}) = 4.1\ \text{m}^3\text{s}^{-1},$$

which corrected for a vesicularity of 0.22 gives a bulk volume flux of,

$$V_R = (1-0.22)(4.1\ \text{m}^3\text{s}^{-1}) = 3.2\ \text{m}^3\text{s}^{-1}.$$

We thus found that, over five hours, the volume flux was somewhat variable, where increases in the flux were sometimes quite obvious from the passage of a "wave" of lava down the channel, the passage of which caused lava to overflow the channel for a few minutes, "normal" and "overflowing" flow conditions being pictured in Figure S7.5.

Given that the volume fluxes measured in the field were variable over the time scale of minutes to hours, but were generally in the range 0.6 $m^3\ s^{-1}$ to 3.2 $m^3\ s^{-1}$, the result given in the answer keys of Table S7.4 and Table S7.5, i.e., 2.5 – 3.0 $m^3\ s^{-1}$ for 29 May and 1.7 – 2.0 $m^3\ s^{-1}$ for 30 May look good. That is, the results fall within the field-derived range of flux variation. Fluxes were variable over the time scale of minutes, about a mean and standard deviation of 1.7±0.5 $m^3\ s^{-1}$, making the satellite-derived result plausible. In fact, the satellite data suggest that the 29 May image was acquired during a period when the flow field was responding to a pulse (or peak) in the erupted volume flux, and the 30 May image during a period of "normal" supply.

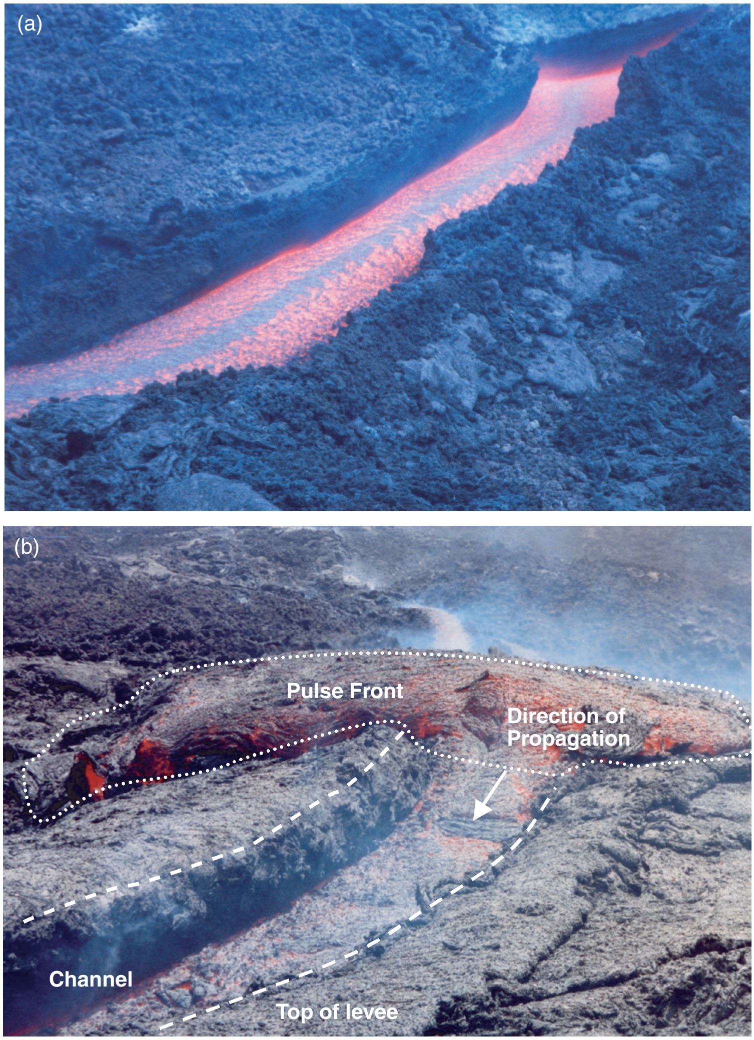

Figure S7.5 Photo of the proximal section of the lava channel that fed flows active on Mt. Etna during 30 May 2001. This channel was active in the pixels of the AVHRR images of Figures S7.1 and S7.2, and was ~3 m wide. In (a) it is pictured flowing during “normal” flow conditions, and in (b) during “overflowing” flow conditions when high volume flux pulses propagated down the channel. Pulses were apparent as a wave which, in this pictured case, was ~1.5 m high. Bailey *et al*. (2006) provides a full and detailed description of activity across this lava flow field during the time of image acquisition.

References

Bailey, J. E., Harris, A. J. L., Dehn, J., Calvari, S. and Rowland, S. K. (2006). The changing morphology of an open lava channel on Mt. Etna. *Bulletin of Volcanology*, **68**, 497–515.

Harris, A. J. L., Dehn, J. and Calvari, S. (2007). Lava Effusion Rate Definition and Measurement: A Review. *Bulletin of Volcanology*, **70**, 1–22.

Wright, R., Blake, S., Harris, A. and Rothery, D. (2001). A simple explanation for the space-based calculation of lava eruptions rates. *Earth and Planetary Science Letters*, **192**, 223–233.